Available online at www.sciencedirect.com
ScienceDirect
Trans. Nonferrous Met. Soc. China 35(2025) 338−348
Transactions of Nonferrous Metals Society of China
www.tnmsc.cn

Phase equilibria of slag systems "FeO"−SiO_2−CaO−Al_2O_3 and "FeO" −SiO_2−CaO−MgO at 1200 °C and $p(O_2)$ of 10^{-7} kPa

Sui XIE[1,2], Qin-meng WANG[3], Xue-yi GUO[3], Chun-fa LIAO[1], Bao-jun ZHAO[1,2,4]

1. Faculty of Materials, Metallurgy and Chemistry, Jiangxi University of Science and Technology, Ganzhou 341000, China;
2. National Rare Earth Functional Material Innovation Center, Ganzhou 341000, China;
3. School of Metallurgy and Environment, Central South University, Changsha 410083, China;
4. Sustainable Minerals Institute, The University of Queensland, Brisbane 4072, Australia

Received 7 June 2023; accepted 11 November 2023

Abstract: High-temperature experiments were carried out for the slag systems of "FeO"−SiO_2−CaO−Al_2O_3 and "FeO"−SiO_2−CaO−MgO at 1200 °C and $p(O_2)$ of 10^{-7} kPa. The equilibrated samples were quenched, and the phase compositions were measured by electron probe microanalysis (EPMA). A series of pseudo-ternary and pseudo-binary phase diagrams are constructed to demonstrate their applications in copper smelting process and evaluation of the thermodynamic database. Spinel and tridymite are identified to be the major primary phases in the composition range related to the copper smelting slags. It is found that the operating window of the smelting slag is primarily determined by w_{Fe}/w_{SiO_2} ratio in the slag. Both MgO and Al_2O_3 in the slag reduce the operating window which requires extra fluxing agent to keep the slag to be fully liquid. Complex spinel solid solutions cause inaccurate predictions of the current thermodynamic database.

Key words: phase equilibrium; "FeO"−SiO_2−CaO−Al_2O_3 slag system; "FeO"−SiO_2−CaO−MgO slag system; oxygen partial pressure; copper smelting slag; FactSage

1 Introduction

Copper mainly exists in the earth's crust in the form of copper−iron−sulfide. Approximately 85% of primary copper is produced through pyro-metallurgical process, which involves copper concentrate smelting, matte converting, and refining processes [1−3]. In the smelting process, copper concentrates react with oxygen and flux to produce matte with 50−75 wt.% Cu, SO_2-containing gas, and oxide slag. The oxygen partial pressure in the smelting process ranges from 10^{-5} to 10^{-7} kPa depending on the matte grade and smelting temperature [4−6]. The bottom-blowing smelting (BBS) process developed in China has the advantages of good adaptability to raw materials, high oxygen utilization, high thermal efficiency, and flexible capacity, making it suitable for treating low-grade copper concentrates [7,8]. Low-temperature and low-$p(O_2)$ are the features of the BBS slag because of low-grade copper concentrates treatment. The liquidus temperatures of the smelting slag are directly related to the Fe^{3+}/Fe^{2+} ratio which is controlled as a function of oxygen partial pressure [9−12]. Impurities such as MgO, Al_2O_3, and CaO are increasingly present in the copper smelting slag due to the utilization of low-grade copper concentrates [13]. These impurities, as well as oxygen partial pressure, play a significant

Corresponding author: Bao-jun ZHAO, E-mail: bzhao@jxust.edu.cn
https://doi.org/10.1016/S1003-6326(24)66683-5

role in the physicochemical properties of the slag such as liquidus temperature and viscosity [14−16]. The physicochemical properties of the slag directly affect the stable operation, copper recovery, and thermal efficiency in the smelting process [17].

"FeO"−SiO_2−CaO is a basic slag system in nonferrous smelting process. Several studies have determined the phase equilibria of the system FeO−Fe_2O_3−SiO_2−CaO at iron saturation [18−20], in air [21,22], and in intermediate oxygen partial pressures [23−25]. HIDAYAT et al [24,25] reported the phase equilibria of the system FeO−Fe_2O_3−SiO_2−CaO at $p(O_2)$ of 10^{-4}−10^{-7} kPa. It was found that spinel and tridymite are the primary phases at $p(O_2)$ of 10^{-7} kPa and 1200 °C. The fully liquid area at 1200 °C significantly decreased with increasing oxygen partial pressure. ZHAO et al [26,27] investigated the liquidus temperatures in the system "FeO"−SiO_2−CaO−Al_2O_3−MgO at iron saturation. The liquidus temperatures of the slag in the olivine primary phase field were found to increase with increasing MgO content and decrease with increasing Al_2O_3 content. HENAO et al [28] studied the phase equilibria of the system "FeO"−SiO_2−MgO at constant 3.3 wt.% CaO and 3.3 wt.% Al_2O_3, $p(O_2)$ of 10^{-6} kPa, and 1250−1350 °C. An optimization procedure was introduced to obtain the target concentrations of all components in the liquid phase. No information was found in the systems "FeO"−SiO_2−CaO−Al_2O_3 and "FeO"−SiO_2−CaO−MgO at 1200 °C and $p(O_2)$ of 10^{-7} kPa.

The BBS technology developed in China usually operates at low-temperature and low-$p(O_2)$ when low-grade copper concentrates are treated. This study focuses on the phase equilibria of the systems "FeO"−SiO_2−CaO−Al_2O_3 and "FeO"−SiO_2−CaO−MgO at 1200 °C and $p(O_2)$ of 10^{-7} kPa related to the BBS slags. Pseudo-ternary sections of "FeO"−SiO_2−CaO−Al_2O_3 at constant 2, 4, and 6 wt.% Al_2O_3, and "FeO"−SiO_2−CaO−MgO at constant 2 and 4 wt.% MgO are constructed by high-temperature experiments. The thermodynamic software FactSage 8.2 [29] was used to plan the experiments and the predictions are compared with the experimental results.

2 Experimental

The experimental procedure used in the present study has been described in detail in previous publications [30−37]. The furnace used for equilibration experiments is shown in Fig. 1. Pure powders of Fe_2O_3 (99.99 wt.%), SiO_2 (99.99 wt.%), MgO (99.95 wt.%), Al_2O_3 (99.99 wt.%), Fe (99.9 wt.%) and CaO (calcined at 1000 °C from 99.0 wt.% $CaCO_3$) were mixed and pelletized. Approximately 0.1−0.2 g sample was placed in a Pt envelope (10 mm × 12 mm × 0.025 mm) and equilibrated for 24 h under a CO/CO_2 mixture gas flow (400 mL/min CO_2 and 40 mL/min CO). The output gas from the experimental furnace was periodically introduced to another furnace at the same temperature and equipped with a DS-type oxygen probe to check the oxygen partial pressure. The accuracy of the DS-type oxygen probe is ±0.1lg[$p(O_2)$] units. The compositions of phases present in the quenched sample after equilibration were determined by a JXA 8200 electron probe micro-analyzer (EPMA) with the wavelength dispersive detectors. EMPA was operated at an acceleration voltage of 15 kV and a probe current of 15 nA. The ZAF correction procedure was applied. Fe_2O_3, $CaSiO_3$, Al_2O_3, and MgO were used as standards for Fe, Ca, Si, Al and Mg, respectively.

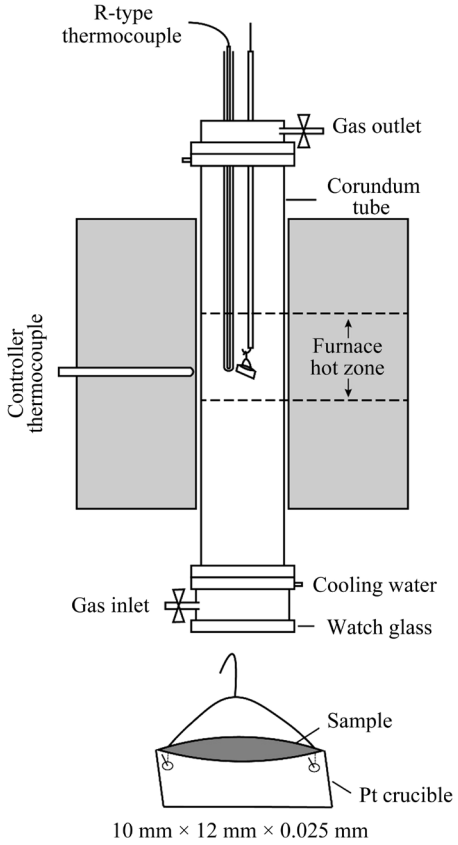

Fig. 1 Schematic of vertical tube furnace for equilibration

FactSage calculations show that the Fe^{2+}/Fe^{3+} is 8−15 in the liquid phase at 1200 °C and $p(O_2)$ of 10^{-7} kPa. All iron oxide was recalculated as "FeO" in this work for presentation purposes.

3 Results and discussion

3.1 Choices of pseudo-ternary sections and $p(O_2)$

To show the effect of impurities (MgO, Al_2O_3, CaO) on liquidus temperatures, the pseudo-ternary sections "FeO"−SiO_2−CaO−Al_2O_3 at constant Al_2O_3 and "FeO"−SiO_2−CaO−MgO at constant MgO concentrations have been projected onto the "FeO"−SiO_2−CaO plane, as shown in Fig. 2.

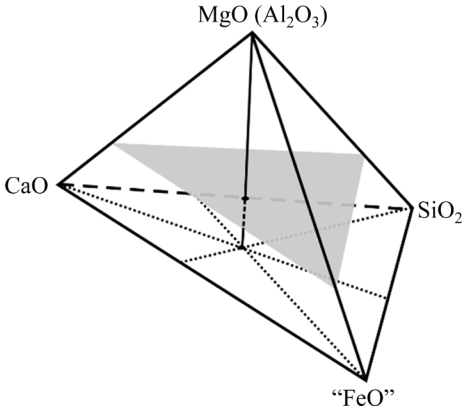

Fig. 2 "FeO"−SiO_2−CaO−Al_2O_3 and "FeO"−SiO_2−CaO−MgO on "FeO"−SiO_2−CaO plane

Matte grade is a function of slag composition, smelting temperature, $p(O_2)$ and $p(SO_2)$. Figure 3 shows the effect of matte grade and $p(SO_2)$ on oxygen partial pressure in equilibrium with slag and tridymite for Cu−Fe−S−O−SiO_2 system, at 1200 °C, calculated by FactSage 8.2. It can be seen that the oxygen partial pressure in the smelting process ranges from $10^{-5.5}$ to $10^{-7.5}$ kPa when the matte grade is in the range of 50−70 wt.% Cu at 1200 °C. The $p(O_2)$ of 10^{-7} kPa was selected to represent the operating conditions at various matte grades and almost constant $p(SO_2)$.

The liquid phase at high temperatures was converted into a uniform glass phase at room temperature through rapid quenching. The compositions of the liquid phase and solid phases can be quantitatively measured by EPMA. Figure 4 shows the typical microstructures of the quenched samples, illustrating that the liquid is in equilibrium with spinel (Fig. 4(a)), SiO_2 (Fig. 4(b)), SiO_2 and $CaSiO_3$ (Fig. 4(c)), and with spinel, SiO_2, and olivine (Fig. 4(d)).

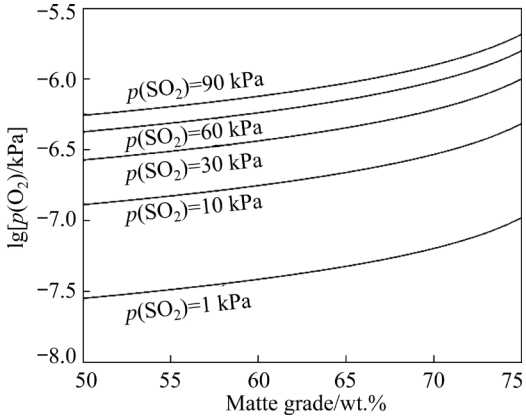

Fig. 3 Effect of matte grade and $p(SO_2)$ on oxygen partial pressure in equilibrium with slag and tridymite for Cu−Fe−S−O−SiO_2 system at 1200 °C calculated by FactSage 8.2

The phase compositions in the quenched samples measured by EPMA are listed in Table 1 ("FeO"−SiO_2−CaO−MgO) and Table 2 ("FeO"−SiO_2−CaO−Al_2O_3). Spinel [$(Fe^{2+},Mg)O\cdot(Al,Fe^{3+})_2O_3$] contains up to 2.4 wt.% MgO, 1.1 wt.% SiO_2, and 7.9 wt.% Al_2O_3. Tridymite (SiO_2) contains up to 1.1 wt.% FeO. Olivine [$(Fe,Mg,Ca)_2SiO_4$] contains up to 31.1 wt.% CaO and 23.2 wt.% MgO.

In the multicomponent systems, the liquid phase after the equilibration may not contain the exact Al_2O_3 and MgO concentrations for the pseudo-ternary sections due to the precipitation of the solid phase This makes it difficult to obtain the liquid with the target MgO or Al_2O_3 concentrations. To address this issue, empirical equations are given in Table 3.

These equations allow the liquid composition with the target MgO or Al_2O_3 concentrations to be calculated based on the experimental data. In the spinel and olivine primary phase fields, the "FeO" concentration in the liquid is a function of CaO, MgO, and Al_2O_3 concentrations in the liquid. In the tridymite primary phase field, the w_{CaO}/w_{SiO_2} ratio in the liquid can be obtained from the "FeO", MgO, and Al_2O_3 concentrations in the liquid. The interpolated points can be calculated by the following equations as an example in spinel primary phase field:

$$w_{\text{"FeO"}} = -1.357w_{MgO} - 1.210w_{Al_2O_3} + 0.0113w_{CaO}^2 - 1.476w_{CaO} + 72.793 \quad (1)$$

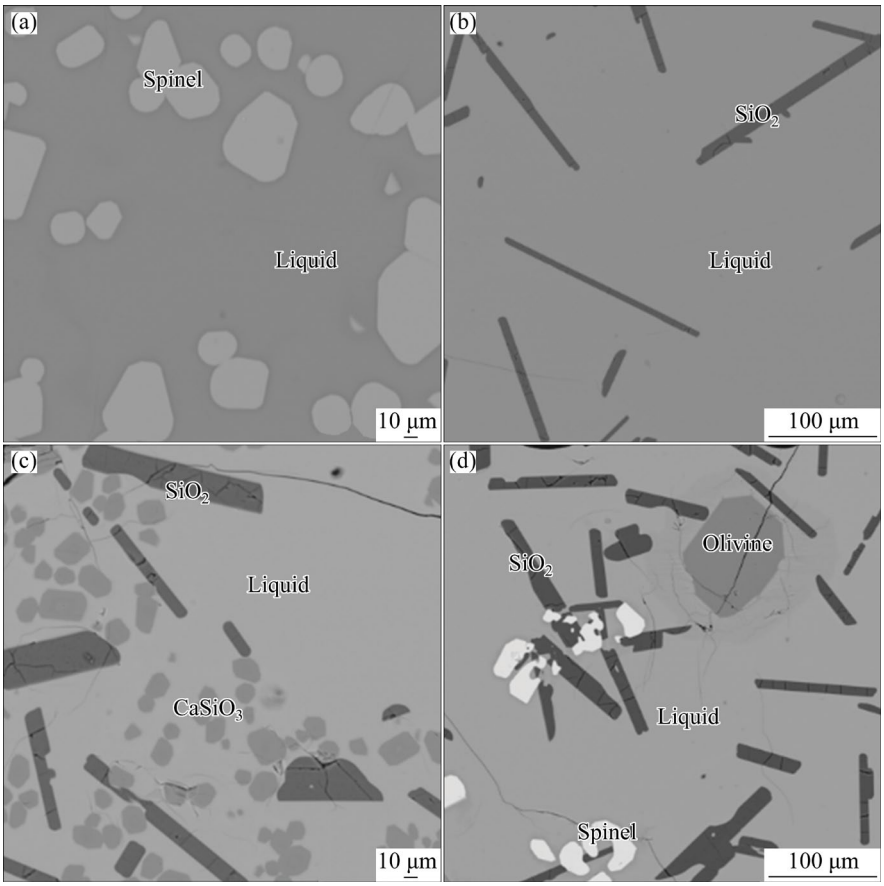

Fig. 4 Typical microstructures of quenched samples showing equilibrium of liquid with spinel (a), SiO_2 (b), $CaSiO_3$ (wollastonite) and SiO_2 (c), and spinel, SiO_2 and olivine (d)

$$w_{\text{"FeO"}} + w_{\text{MgO}} + w_{\text{Al}_2\text{O}_3} + w_{\text{CaO}} + w_{\text{SiO}_2} = 100 \quad (2)$$

Figure 5 shows the examples of the correlations among "FeO", CaO and Al_2O_3 (Fig. 5(a)), and the correlations among "FeO", CaO and MgO (Fig. 5(b)) in the liquid of the spinel primary phase field.

It can be seen from Fig. 6 that the experimental results and the calculated values using the empirical equations agree very well in all major primary phase fields investigated. The empirical equations can be used to obtain the composition of a liquid with the target MgO or Al_2O_3 concentrations. The isotherms at constant MgO or Al_2O_3 concentrations within the investigated composition range can be constructed using the empirical equations.

3.2 1200 °C isotherms in systems "FeO"−SiO_2−CaO−MgO and "FeO"−SiO_2−CaO−Al_2O_3 at $p(O_2)$ of 10^{-7} kPa

Figure 7 shows experimentally determined pseudo-ternary section projected onto the "FeO"−SiO_2−CaO plane at 2 and 4 wt.% MgO at 1200 °C and $p(O_2)$ of 10^{-7} kPa. The isotherms from the system "FeO"−SiO_2−CaO (0 wt.% MgO) are also shown for comparison [25]. When 6 wt.% MgO is present in the slag, liquid phase does not exist in the composition range investigated at 1200 °C and $p(O_2)$ of 10^{-7} kPa. As can be seen from Fig. 7, spinel and tridymite are the primary phases in the system "FeO"−SiO_2−CaO. Addition of MgO in the slag introduces olivine primary phase field in the composition range investigated. The isotherms in the spinel and tridymite primary phase fields move towards a low w_{Fe}/w_{SiO_2} ratio direction with increasing MgO content. The isotherms in the olivine primary phase field move towards a low "FeO" direction with increasing MgO content. Full liquid area surrounded by the isotherms decreases with increasing MgO content until disappears at 6 wt.% MgO. In the copper smelting process, SiO_2 is commonly used as a flux (represented by w_{Fe}/w_{SiO_2} ratio) to control the slag composition to obtain a required liquidus temperature. A fully liquid area

Table 1 Phase compositions in quenched samples in "FeO"−CaO−SiO_2−MgO system at 1200 °C and $p(O_2)$ of 10^{-7} kPa (EPMA, wt.%)

No.	Phase	Composition				No.	Phase	Composition			
		"FeO"	CaO	SiO_2	MgO			"FeO"	CaO	SiO_2	MgO
1	Liquid	39.5	24.5	33.1	2.9	11	Liquid	39.4	10.6	45.8	4.2
	Spinel	98.5	0.0	0.2	1.3		SiO_2	0.7	0.0	99.3	0.0
	Olivine	28.3	31.1	33.2	7.5	12	Liquid	41.2	10.9	45.8	2.1
2	Liquid	41.1	20.7	33.5	4.7		SiO_2	0.7	0.1	99.2	0.0
	Spinel	97.6	0.1	0.3	1.9	13	Liquid	51.4	4.1	41.6	2.9
	Olivine	27.4	27.4	33.9	11.3		SiO_2	1.0	0.0	99.0	0.0
3	Liquid	42.3	18.6	34.2	4.9	14	Liquid	56.1	10.7	31.5	1.8
	Spinel	97.6	0.1	0.4	1.9		Spinel	98.9	0.0	0.5	0.5
	Olivine	37.3	4.5	35.1	23.1	15	Liquid	42.5	22.5	33.1	1.8
4	Liquid	64.9	3.9	29.7	1.5		Spinel	98.9	0.1	0.3	0.8
	Spinel	98.7	0.0	0.8	0.4	16	Liquid	53.2	11.1	32.2	3.5
	Olivine	61.6	0.5	31.3	6.6		Spinel	98.3	0.0	0.6	1.1
5	Liquid	62.6	5.0	30.3	2.1	17	Liquid	26.9	19.8	50.1	3.3
	Spinel	98.6	0.0	0.8	0.6		SiO_2	0.5	0.1	99.4	0.0
	Olivine	59.5	0.6	31.6	8.3		$CaSiO_3$	14.9	23.2	51.5	10.3
6	Liquid	58.8	7.9	30.7	2.6	18	Liquid	30.9	16.3	48.4	4.3
	Spinel	98.4	0.0	0.7	0.8		SiO_2	0.6	0.1	99.3	0.0
	Olivine	54.3	1.2	32.2	12.4		$CaSiO_3$	12.0	22.9	51.7	13.4
7	Liquid	41.6	19.6	34.3	4.5	19	Liquid	38.3	9.9	45.3	6.5
	Spinel	96.1	0.4	1.1	2.4		Spinel	97.7	0.0	0.4	1.9
	Olivine	35.8	6.2	34.8	23.2		SiO_2	0.8	0.0	99.2	0.0
8	Liquid	61.5	0.0	36.6	1.9		Pyroxene	24.3	2.8	52.4	20.4
	SiO_2	1.1	0.0	98.9	0.0	20	Liquid	48.8	4.7	41.9	4.6
	Olivine	62.4	0.0	30.9	6.7		SiO_2	0.6	0.0	99.4	0.0
9	Liquid	60.9	0.0	36.6	2.5		Olivine	51.2	0.2	32.7	15.9
	SiO_2	0.9	0.0	99.1	0.0		Pyroxene	32.6	0.7	50.9	15.9
	Olivine	59.8	0.0	31.6	8.6	21	Liquid	33.1	12.4	48.7	5.8
10	Liquid	49.6	4.4	42.3	3.7		Pyroxene	13.4	18.0	52.9	15.7
	SiO_2	0.6	0.0	99.4	0.0		SiO_2	0.5	0.1	99.4	0.0
	Olivine	54.3	0.2	32.6	12.9						

represents the operating window for the variation of the slag composition. As the concentration of MgO in the slag increases, the operating window moves towards high-SiO_2 and high-CaO regions. This suggests that both SiO_2 and CaO are required to obtain a fully liquid slag in the copper smelting process with the increase of MgO concentration in the slag.

The pseudo-ternary phase diagram of "FeO"−SiO_2−CaO−Al_2O_3 at constant 2, 4, and 6 wt.% Al_2O_3 are constructed from the experimental results, as shown in Fig. 8. The liquidus compositions are shown to indicate the composition range investigated. The isotherms without Al_2O_3 are also shown for comparison [25]. Spinel and tridymite are the primary phases with the Al_2O_3

Table 2 Phase compositions in quenched samples for "FeO"−CaO−SiO_2−Al_2O_3 system at 1200 °C and $p(O_2)$ of 10^{-7} kPa (EPMA, wt.%)

No.	Phase	Composition			
		"FeO"	CaO	SiO_2	Al_2O_3
22	Liquid	58.4	0.0	37.9	3.6
	SiO_2	0.9	0.0	99.1	0.0
23	Liquid	53.1	0.0	39.8	7.2
	SiO_2	0.9	0.0	99.1	0.0
24	Liquid	26.8	19.0	50.7	3.5
	SiO_2	0.5	0.1	99.4	0.0
25	Liquid	24.5	17.2	51.9	6.4
	SiO_2	0.5	0.1	99.3	0.1
26	Liquid	69.7	0.0	27.3	2.9
	Spinel	94.4	0.0	0.8	4.8
27	Liquid	65.8	0.0	28.6	5.5
	Spinel	87.3	0.0	0.6	12.0
28	Liquid	41.5	22.4	32.9	3.3
	Spinel	96.3	0.1	0.2	3.3
29	Liquid	37.7	22.7	33.1	6.4
	Spinel	92.6	0.1	0.2	7.0
30	Liquid	54.0	10.9	31.8	3.3
	Spinel	95.9	0.0	0.5	3.5
31	Liquid	49.9	11.1	32.7	6.3
	Spinel	91.6	0.0	0.4	7.9
32	Liquid	40.4	10.6	45.2	3.9
	Spinel	98.6	0.0	0.0	1.4
	SiO_2	1.0	0.1	98.9	0.0
33	Liquid	33.9	10.4	48.1	7.5
	Spinel	96.8	0.0	0.3	2.9
	SiO_2	0.6	0.1	99.2	0.1

concentrations from 0 to 6 wt.% at 1200 °C and $p(O_2)$ of 10^{-7} kPa. As shown in Fig. 8, the isotherms in both spinel and tridymite primary phase fields move towards a high w_{Fe}/w_{SiO_2} direction with increasing Al_2O_3 content in the slag. The fully liquid area moves accordingly with the isotherms, but the size of the fully liquid area does not change with the Al_2O_3 content. SiO_2 needs to be increased to obtain a full-liquid slag with the increased Al_2O_3 concentration in the slag.

Table 3 Empirical equations in different primary phase fields

Primary phase	Empirical equations
Spinel	$w_{\text{"FeO"}}=-1.357w_{MgO}-1.210w_{Al_2O_3}+0.0113w_{CaO}^2-1.476w_{CaO}+72.793$
SiO_2	$\frac{w_{CaO}}{w_{SiO_2}}=-0.0178w_{MgO}-0.0199w_{Al_2O_3}-0.0000391w_{\text{"FeO"}}^2-0.00844w_{FeO}+0.699$
Olivine	$w_{\text{"FeO"}}=-3.410w_{MgO}+0.000267w_{Al_2O_3}-0.0418w_{CaO}^2+0.237w_{CaO}+68.923$

$w_{\text{"FeO"}}$, w_{SiO_2}, w_{CaO}, w_{MgO}, and $w_{Al_2O_3}$ are mass fractions of "FeO", SiO_2, CaO, MgO and Al_2O_3 in liquid, respectively

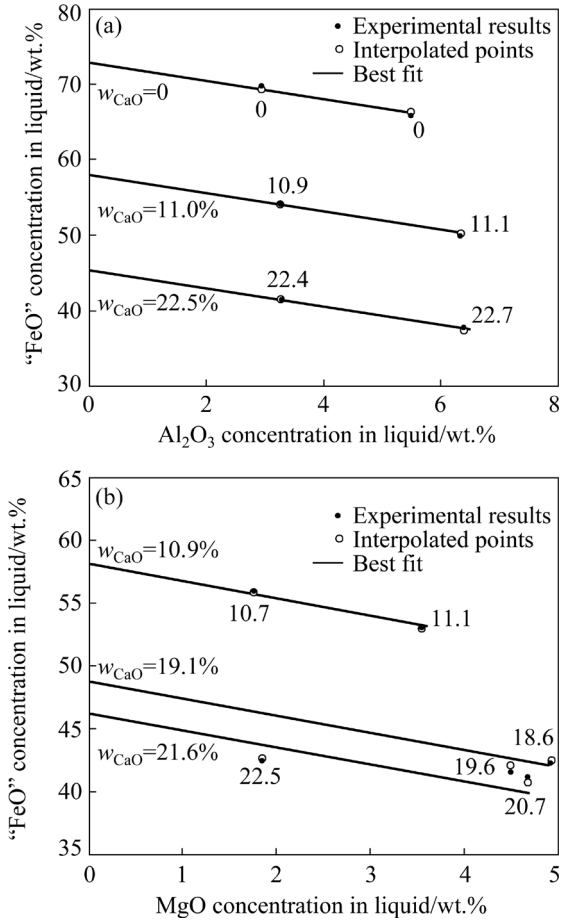

Fig. 5 Correlations between "FeO", CaO and Al_2O_3 or MgO concentrations in liquid in equilibrium with spinel, at 1200 °C and $p(O_2)$ of 10^{-7} kPa

Figure 9 compares the effects of MgO and Al_2O_3 on the 1200 °C isotherms at $p(O_2)$ of 10^{-7} kPa. It can be seen that, addition of 4 wt.% of MgO or Al_2O_3 moves the isotherms to the same position in the spinel and tridymite primary phase fields. However, olivine phase is introduced with 4 wt.%

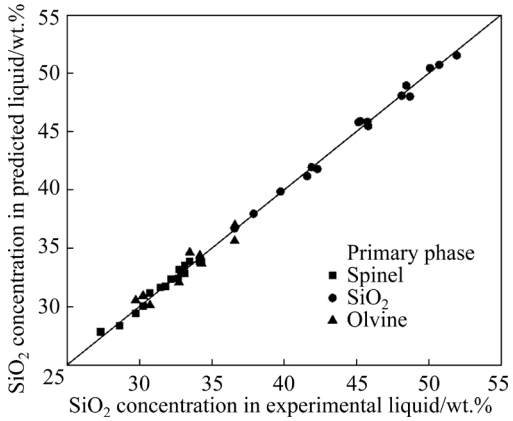

Fig. 6 Comparison between experimental results and calculated results using empirical equations

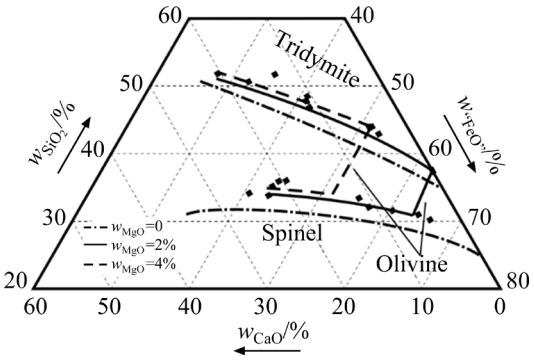

Fig. 7 Experimentally determined pseudo-ternary section projected on "FeO"−SiO_2−CaO plane with 2 and 4 wt.% MgO at 1200 °C and $p(O_2)$ of 10^{-7} kPa (0 wt.% MgO isotherms are from Ref. [25])

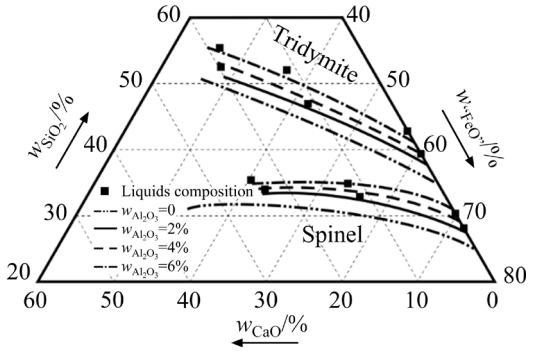

Fig. 8 Experimentally determined pseudo-ternary section projected on "FeO"−SiO_2−CaO plane with 2, 4, 6 wt.% Al_2O_3 at 1200 °C and $p(O_2)$ 10^{-7} kPa (0 wt.% Al_2O_3 isotherms are from [25])

MgO addition, which results in a much smaller fully liquid area than that with 4 wt.% Al_2O_3. Not only SiO_2 but also CaO is required to obtain a fully liquid slag when 4 wt.% MgO is present in the slag.

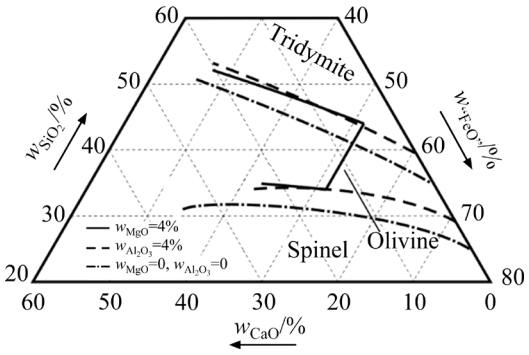

Fig. 9 Comparison of effects of MgO and Al_2O_3 on isotherms (0 wt.% Al_2O_3 and MgO isotherms are from Ref. [25])

3.3 Difference between FactSage predictions and experimental results

FactSage 8.2 software, powerful thermodynamic computer package, was used to predict the phase equilibria of the systems "FeO"−SiO_2−CaO−MgO and "FeO"−SiO_2−CaO−Al_2O_3 under the same conditions as the experiments [29]. The databases selected were "FactPS" and "FToxid". The solution phases selected included "FToxid-SLAGA," "FToxid-SPINC," "FToxid-MeO_A," "FToxid-cPyrA," "FToxid-oPyrA," "FToxid-pPyrA," "FToxid-LcPy," "FToxid-WOLLA," "FToxid-Mel_A," "FToxid-OlivA," "FToxid-Mull," and "FToxid-CORU." As shown in Fig. 10(a), the primary phases predicted by FactSage are the same as the experimental results when 4 wt.% Al_2O_3 is present in the slag. FactSage predicts a slightly larger full liquid area than the experimental one. On the other hand, it can be seen from Fig. 10(b) that the fully liquid area when 4 wt.% MgO is present in the slag. According to the FactSage predictions, the spinel phase does not appear with up to 20 wt.% CaO. A small $CaSiO_3$ primary phase field appears at low-CaO content area. The isotherm in the olivine primary phase field is predicted to be in around 40 wt.% "FeO" compared to that in 51 wt.% "FeO" from the experimental data. As a result, the predicted fully liquid area of the slag is much smaller than that determined by experimental results.

The slag composition is usually adjusted by the w_{Fe}/w_{SiO_2} ratio in the copper smelting process. The range of the w_{Fe}/w_{SiO_2} ratio to obtain a fully liquid slag is defined as operating window of slag composition. Figure 11 shows the effect of

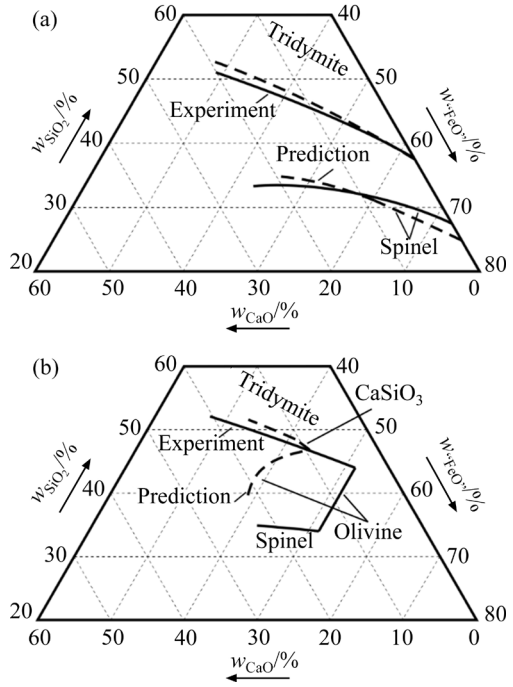

Fig. 10 Comparison of experimental results with FactSage predictions at 1200 °C and $p(O_2)$ of 10^{-7} kPa: (a) 4 wt.% Al_2O_3; (b) 4 wt.% MgO

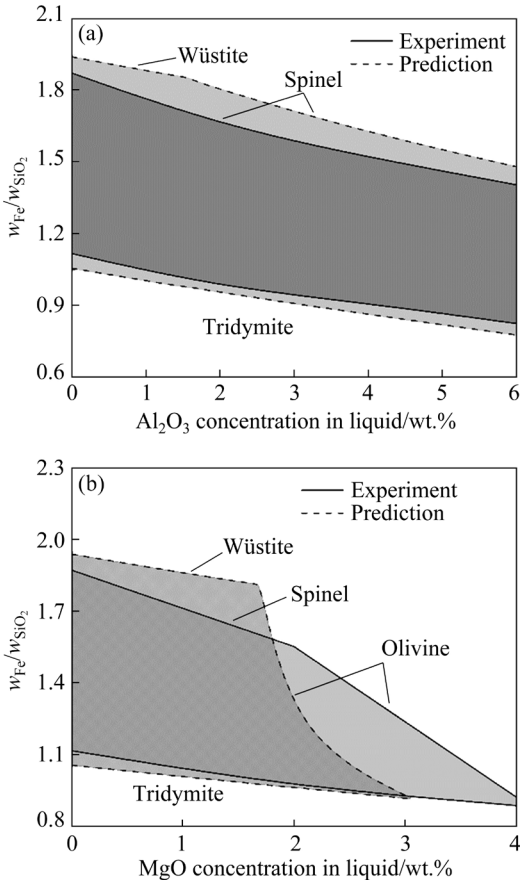

Fig. 11 Effect of impurities on w_{Fe}/w_{SiO_2} range of full liquid at 5 wt.% CaO with comparison between experimental results and FactSage predictions

impurities (MgO or Al_2O_3) on w_{Fe}/w_{SiO_2} range to obtain a fully liquid slag at 5 wt.% CaO. As can be seen from Figs. 11(a, b), FactSage predicts the existence of a Wüstite primary phase field at Al_2O_3 or MgO up to 2 wt.%. Wüstite is not found in the experimental study. As shown in Fig. 11(a), w_{Fe}/w_{SiO_2} ratio needs to be reduced to obtain a fully liquid slag when the Al_2O_3 concentration in the slag is increased. The range of the w_{Fe}/w_{SiO_2} ratio decreases with increasing Al_2O_3 concentration in the slag. The experimentally determined operating window (range of the w_{Fe}/w_{SiO_2} ratio) is smaller than that predicted by the FactSage.

From Fig. 11(b), it can be seen that the slag operating window decreases significantly with increasing MgO concentration as the primary phase field changes from spinel to olivine. FactSage predicts the same trend as the experimental results but different values. For example, a fully liquid slag can be obtained by controlling the w_{Fe}/w_{SiO_2} ratio in the range of 0.9−1.3 when 3 wt.% MgO is present. However, FactSage does not predict the presence of the fully liquid slag under the same condition.

3.4 Distribution of MgO and Al_2O_3 between spinel and liquid phases

Figures 10 and 11 show that the experimental results are different from the FactSage predictions, in particular, in the primary phase fields of iron oxides (spinel and wüstite). The accuracy of the calculations depends on the reliable thermodynamic database which is developed from the accurate experimental data. Figures 12 and 13 show the distribution of MgO and Al_2O_3 between the spinel

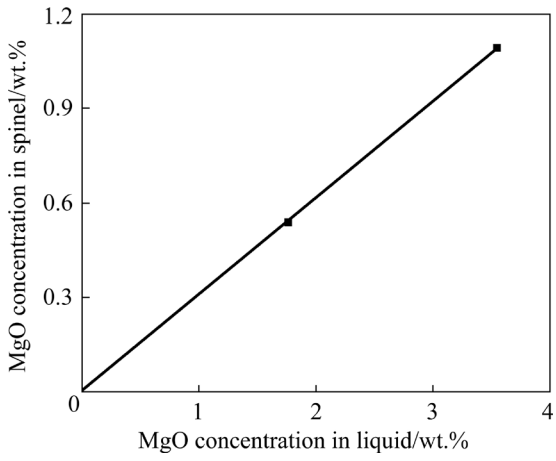

Fig. 12 Distribution of MgO between spinel and liquid phases at w_{CaO}/w_{SiO_2} ratio of 0.34 in liquid, 1200 °C and $p(O_2)$ of 10^{-7} kPa

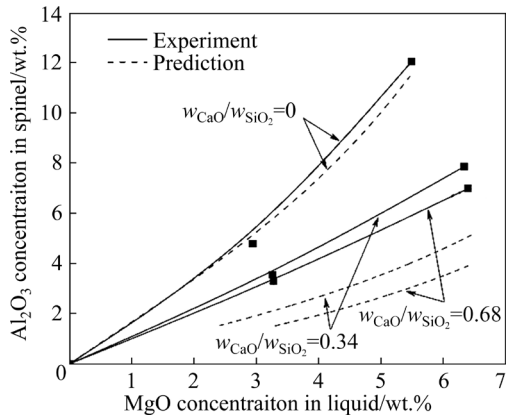

Fig. 13 Distribution of Al_2O_3 concentration between spinel and liquid phases, at 1200 °C and $p(O_2)$ of 10^{-7} kPa

and liquid phases which gives the direction for the optimization of the thermodynamic database. FactSage does not predict the existence of the spinel when MgO is present in the slag. Figure 12 shows the experimentally determined distribution of MgO between spinel and liquid phases at a constant w_{CaO}/w_{SiO_2} ratio of 0.34 in the liquid. It can be seen that MgO concentrations in the spinel solid solution increase with increasing MgO concentration in the liquid. The MgO concentration in the spinel is approximately 30 wt.% of that in the liquid.

Figure 13 shows the distribution of Al_2O_3 between spinel and liquid phases at different w_{CaO}/w_{SiO_2} ratios in the liquid. The dashed lines at w_{CaO}/w_{SiO_2} ratios of 0.34 and 0.68 do not appear at low-Al_2O_3 concentration because Wüstite is predicted by FactSage 8.2. It can be seen that, at a constant w_{CaO}/w_{SiO_2} ratio, the concentration of Al_2O_3 in the spinel increases with increasing Al_2O_3 concentration in the liquid. High w_{CaO}/w_{SiO_2} ratio in the liquid results in a lower Al_2O_3 concentration in the spinel at the same Al_2O_3 concentration in the liquid. FactSage predicts the same trends as the experimental results. In the CaO-free slag (w_{CaO}/w_{SiO_2}=0), the predictions are close to the experimental data. However, at w_{CaO}/w_{SiO_2} ratios of 0.34 and 0.68 in the liquid, FactSage predicts a much lower Al_2O_3 concentration in the spinel. The difference between the calculated and experimental results increases with increasing w_{CaO}/w_{SiO_2} ratio. For instance, at 4 wt.% Al_2O_3 in the liquid, the difference between the predictions and experimental results is 2.0 and 2.3 at w_{CaO}/w_{SiO_2} ratio of 0.34 and 0.69, respectively.

4 Conclusions

(1) The primary phases are identified to be spinel, tridymite, and olivine. The isotherms in the spinel and tridymite primary phase fields move to the high-SiO_2 concentration direction with increasing MgO and Al_2O_3 concentrations in the slag.

(2) w_{Fe}/w_{SiO_2} range of full liquid decreases with increasing MgO and Al_2O_3 concentrations. More SiO_2 flux is required to obtain a fully liquid slag with the increase of MgO and Al_2O_3 concentrations in the slag.

(3) FactSage predicts the same tendency as the experimental results. Significant differences between the experimental results and FactSage predictions on primary phase and isotherm position can be attributed to the inaccurate solid solution compositions in the current thermodynamic database.

CRediT authorship contribution statement

Sui XIE: Methodology and experiments, Data analyses, Original draft; **Qin-meng WANG:** Writing – Review & editing; **Xue-yi GUO:** Writing – Review & editing; **Chun-fa LIAO:** Writing – Review & editing; **Bao-jun ZhAO:** Methodology and experiments, Data analyses, Writing – Review & editing.

Declaration of competing interest

The authors declare that they have no known competing financial interests or personal relationships that could have appeared to influence the work reported in this paper.

References

[1] SUN Yong-qi, CHEN Mao, CUI Zhi-xiang, CONTRERAS Leonel, ZHAO Bao-jun. Phase equilibrium studies of iron silicate slag under direct to blister copper-making condition [J]. Metallurgical and Materials Transactions B, 2020, 51: 1−5. https://doi.org/10.1007/s11663-019-01744-4.

[2] XIE Sui, YUAN Xin-hua, LIU Fu-peng, ZHAO Bao-jun. Control of copper content in flash smelting slag and the recovery of valuable metals from slag—A thermodynamic consideration [J]. Metals, 2023, 13(1): 153. https://doi.org/10.3390/met13010153.

[3] GUO Xue-yi, CHEN Yuan-lin, WANG Qin-meng, WANG Song-song, TIAN Qing-hua. Copper and arsenic substance flow analysis of pyrometallurgical process for copper production [J]. Transactions of Nonferrous Metals Society of China, 2022, 32(1): 364−376. https://doi.org/10.1016/S1003-

6326(22)65801-1.

[4] SCHLESINGER M E, SOLE K C, DAVENPORT W G, ALVEAR FLORES G R F. Extractive metallurgy of copper [M]. 8th ed. Oxford: Elsevier, 2021. https://doi.org/10.1016/C2019- 0-03265-7.

[5] HENAO H M, KONGOLI F, ITAGAKI K. High temperature phase relations in FeO_X (X=1 and 1.33)−CaO−SiO_2 systems under various oxygen partial pressure [J]. Materials Transactions, 2005, 46(4): 812−819. https://doi.org/10.2320/matertrans.46.812.

[6] SHISHIN D, HIDAYAT T, FALLAH-MEHRJARDI A, HAYES P C, DECTEROV S A, JAK E. Integrated experimental and thermodynamic modeling study of the effects of Al_2O_3, CaO, and MgO on slag-matte equilibria in the Cu−Fe−O−S−Si−(Al,Ca,Mg) system [J]. Journal of Phase Equilibria and Diffusion, 2019, 40: 445−461. https://doi.org/10.1007/s11669-019-00716-

[7] ZHAO Bao-jun, LIAO Jin-fa. Development of bottom-blowing copper smelting technology: A review [J]. Metals, 2022, 12(2): 190. https://doi.org/10.3390/met12020190.

[8] WANG Qin-meng, GUO Xue-yi, WANG Song-song, LIAO Li-le, TIAN Qing-hua. Multiphase equilibrium modeling of oxygen bottom-blown copper smelting process [J]. Transactions of Nonferrous Metals Society of China, 2017, 27(11): 2503−2511. https://doi.org/10.1016/S1003-6326(17)60277-2.

[9] BOWEN N.L, SCHAIRER J.F. The system, FeO−SiO_2 [J]. American Journal of Science, 1932, 5(141): 177−213. https://doi.org/10.2475/ajs.s5-24.141.177.

[10] MUAN A. Phase equilibria at high temperatures in oxide systems involving changes in oxidation states [J]. American Journal of Science, 1958, 256(3): 171−207. https://doi.org/10.2475/ajs.256.3.171.

[11] MUAN A. Phase equilibria in the system FeO−Fe_2O_3−SiO_2 [J]. JOM, 1955, 7: 965−976. https://doi.org/10.1007/BF03377595

[12] DARKEN L S. Melting points of iron oxides on silica: Phase equilibria in the system Fe−Si−O as a function of gas composition and temperature [J]. Journal of the American Chemical Society, 1948, 70(6): 2046−2053. https://doi.org/10.1021/ja01186a019.

[13] GUO Xue-yi, JIANG Bao-cheng, WANG Qin-meng, WANG Song-song, TIAN Qing-hua, LI Dong. Research progress in the simulation of oxygen bottom-blowing copper smelting [J]. Nonferrous Metals Science and Engineering, 2022, 13(3): 9−19. https://doi.org/10.13264/j.cnki.ysjskx.2022.03.002.

[14] CHEN Mao, RAGHUNATH S, ZHAO Bao-jun. Viscosity measurements of SiO_2−"FeO"−MgO system in equilibrium with metallic Fe [J]. Metallurgical and Materials Transactions B, 2014, 45: 58−65. https://doi.org/10.1007/s11663-013-9917-6.

[15] ZHAO Bao-jun, XIE Sui, Li Ming-zhou. Study on slag-matte-gas equilibrium in copper flash smelting process [J]. Nonferrous Metals (Extractive Metallurgy), 2022, 3: 38−43. https://doi.org/10.3969/j.issn.1007-7545.2022.03.006.

[16] WANG Song-song, WANG Qin-meng, GUO Xue-yi, TAN Ke-qin. Operation and fundamentals of direct anode copper production from matte [J]. Metallurgical and Materials Transactions B, 2023, 54: 487−498. https://doi.org/10.1007/s11663-023-02721-8.

[17] CHEN Mao, RAGHUNATH S, ZHAO Bao-jun. Viscosity measurements of "FeO"−SiO_2 slag in equilibrium with metallic Fe [J]. Metallurgical and Materials Transactions B, 2013, 44: 506−515. https://doi.org/10.1007/s11663-013-9810-3.

[18] BOWEN N L, SCHAIRER J F, POSNJAK E. The system, CaO−FeO−SiO_2 [J]. American Journal of Science, 1933, 5(153): 193−284. https://doi.org/10.2475/ajs.s5-26.153.193.

[19] ALLEN W C, SNOW R B. The orthosilicate−iron oxide portion of the system CaO−"FeO"−SiO_2 [J]. Journal of the American Ceramic Society, 1955, 38(8): 264−272. https://doi.org/10.1111/j.1151-2916.1955.tb14944.x.

[20] NAKAMURA S, TSUKIHASHI F, SANO N. Phosphorus partition between $CaO_{satd.}$−BaO−SiO_2−Fe_tO slags and liquid iron at 1873 K [J]. ISIJ International, 1993, 33(1): 53−58. https://doi.org/10.2355/isijinternational.33.53.

[21] PHILLIPS B, MUAN A. Phase equilibria in the system CaO−iron oxide−SiO_2, in air [J]. Journal of the American Ceramic Society, 1959, 42(9): 413−423. https://doi.org/10.1111/ j. 1151-2916.1959.tb12966.x.

[22] NIKOLIC S HENAO H, HAYES P C, JAK E. Phase equilibria in ferrous calcium silicate slags. Part II: Evaluation of experimental data and computer thermodynamic models [J]. Metallurgical and Materials Transactions B, 2008, 39: 189−199. https://doi.org/10.1007/s11663-008-9131-0.

[23] NIKOLIC S, HAYES P C, JAK E. Phase equilibria in ferrous calcium silicate slags. Part I: Intermediate oxygen partial pressures in the temperature range 1200 °C to 1350 °C [J]. Metallurgical and Materials Transactions B, 2008, 39: 179−188. https://doi.org/10.1007/s11663-008-9130-1.

[24] HIDAYAT T, HAYES P C, JAK E. Experimental study of ferrous calcium silicate slags: Phase equilibria at P_{O_2} between 10^{-5} atm and 10^{-7} atm [J]. Metallurgical and Materials Transactions B, 2012, 43: 14−26. https://doi.org/10.1007/s11663-011-9569-3.

[25] HIDAYAT T, HAYES P C, JAK E. Experimental study of ferrous calcium silicate slags: Phase equilibria at P_{O_2} between 10^{-8} atm and 10^{-9} atm [J]. Metallurgical and Materials Transactions B, 2012, 43: 27−38. https://doi.org/10.1007/s11663-011-9572-8.

[26] ZHAO Bao-jun, JAK E HAYES P C. The effect of Al_2O_3 on liquidus temperatures of fayalite slags [J]. Metallurgical and Materials Transactions B, 1999, 30: 597−605. https://doi.org/10.1007/s11663-999-0020-y.

[27] ZHAO Bao-jun, JAK E, HAYES P C. The effect of MgO on liquidus temperatures of fayalite slags [J]. Metallurgical and Materials Transactions B, 1999, 30: 1017−1026. https://doi.org/10.1007/s11663-999-0107-5.

[28] HENAO H M, NEXHIP C, GEORGE-KENNEDY D P, HAYES P C, JAK E. Investigation of liquidus temperatures and phase equilibria of copper smelting slags in the FeO−Fe_2O_3−SiO_2−CaO−MgO−Al_2O_3 system at P_{O_2} 10^{-8} atm [J]. Metallurgical and Materials Transactions B, 2010, 41: 767−779. https://doi.org/10.1007/s11663-010-9369-1.

[29] BALE C W, BELISLE E, CHARTRAND P, DECTEROV S A, ERIKSSON G, GHERIBI A, HACK K, JUNG I H, KANG Y B, MELANCON J, PELTON A D, PETERSEN S, ROBELIN C, SANGSTER J, SPENCER P, van ENDE M A.

Reprint of: FactSage thermochemical software and databases, 2010—2016 [J]. Calphad, 2016, 55: 1−19. https://doi.org/10.1016/j.calphad.2016.07.004.

[30] CHEN Mao, SUN Yong-qi, BALLADARES E, PIZARRO C, ZHAO Bao-jun. Experimental studies of liquid/spinel/matte/gas equilibria in the Si−Fe−O−Cu−S system at controlled $P(SO_2)$ 0.3 and 0.6 atm [J]. Calphad, 2019, 66: 101642. https://doi.org/10.1016/j.calphad.2019.101642.

[31] SUN Yong-qi, CHEN Mao, CUI Zhi-xiang, CONTRERAS L, ZHAO Bao-jun. Development of ferrous-calcium silicate slag for the direct to blister copper-making process and the equilibria investigation [J]. Metallurgical and Materials Transactions B, 2020, 51: 973−984. https://doi.org/10.1007/s11663-020-01817-9.

[32] LIU Hong-quan, CUI Zhi-xiang, CHEN Mao, ZHAO Bao-jun. Phase equilibrium study of ZnO−"FeO"−SiO_2 system at fixed Po_2 10^{-8} atm [J]. Metallurgical and Materials Transactions B, 2016, 47: 164−173. https://doi.org/10.1007/s11663-016-0596-y.

[33] SHISHIN D, MEHRJARDI A, SCHEVCHENKO M, HIDAYAT T, JAK E. Experimental study, thermodynamic calculations and industrial implications of slag/matte/metal equilibria in the Cu−Pb−Fe−O−S−Si system [J]. Journal of Materials Research and Technology, 2022, 19: 899−912. https://doi.org/10.1016/j.jmrt.2022.05.058.

[34] SINEVA S, SHISHIN D, SCHEVCHENKO M, HAYES P C, JAK E. Experimental study and thermodynamic modeling of distribution of elements among slag, matte and metal in the Cu−Fe−O−S−Si−(Zn)−(Al,Ca,Mg) system for copper slag cleaning applications [J]. Journal of Materials Research and Technology, 2023, 23: 5280−5300. https://doi.org/10.1016/j.jmrt.2023.02.120.

[35] SUN Yong-qi, CHEN Mao, CUI Zhi-xiang, CONTRERAS L, ZHAO Bao-jun. Equilibria of iron silicate slags for continuous converting copper-making process based on phase transformations [J]. Metallurgical and Materials Transactions B, 2020, 51: 2039−2045. https://doi.org/10.1007/s11663-020-01901-0.

[36] SUN Yong-qi, CHEN Mao, BALLADARES E, PIZARRO C, CONTRERAS L, ZHAO Bao-jun. Effect of MgO on the liquid/spinel/matte/gas equilibria in the Si−Fe−Mg−O−Cu−S system at controlled $P(SO_2)$ 0.3 and 0.6 atm [J]. Calphad, 2020, 70: 101803. https://doi.org/10.1016/j.calphad.2020.101803

[37] SUN Yong-qi, CHEN Mao, CUI Zhi-xiang, CONTRERAS L, ZHAO Bao-jun. Phase equilibria of ferrous-calcium silicate slags in the liquid/spinel/white metal/gas system for the copper converting process [J]. Metallurgical and Materials Transactions B, 2020, 51: 2012−2020. https://doi.org/10.1007/s11663-020-01887-9

1200 °C、$p(O_2)$为 10^{-7} kPa 条件下"FeO"−SiO_2−CaO−MgO 和"FeO"−SiO_2−CaO−Al_2O_3 渣系的相平衡

谢 岁[1,2]，王亲猛[3]，郭学益[3]，廖春发[1]，赵宝军[1,2,4]

1. 江西理工大学 材料冶金化学学部，赣州 341000；
2. 国家稀土功能材料创新中心，赣州 341000；
3. 中南大学 冶金与环境学院，长沙 410083；
4. Sustainable Minerals Institute, The University of Queensland, Brisbane 4072, Australia

摘 要：在 1200 ℃、$p(O_2)$为 10^{-7} kPa 条件下，对"FeO"−SiO_2−CaO−Al_2O_3 和"FeO"−SiO_2−CaO−MgO 四元渣系进行高温相平衡实验，并将平衡后的样品进行冷淬，通过电子探针(EPMA)测定平衡相成分。构建一系列伪三元及伪二元相图，讨论这些相图在铜冶炼及评估热力学数据库过程中的应用。结果表明，铜冶炼渣成分主要位于尖晶石和 SiO_2 初晶相区。炼渣的操作窗口主要由渣中 $w(Fe)/w(SiO_2)$决定。渣含 MgO 及 Al_2O_3 均会缩小调节渣成分的操作窗口，需要添加额外的助熔剂以保持渣为纯液相。复杂的尖晶石固溶体相导致热力学数据库预测结果不准确。

关键词：相平衡；"FeO"−SiO_2−CaO−Al_2O_3 渣系；"FeO"−SiO_2−CaO−MgO 渣系；氧分压；铜熔炼渣；FactSage

(Edited by Bing YANG)